Quantum fluctuations in the collective 0^+ states of deformed nuclei

Fang-Qi Chen,[1] Yang Sun,[1,2,*] and Peter Ring[3]
[1]*Department of Physics and Astronomy, Shanghai Jiao Tong University, Shanghai 200240, People's Republic of China*
[2]*Institute of Modern Physics, Chinese Academy of Sciences, Lanzhou 730000, People's Republic of China*
[3]*Physik-Department der Technischen Universität München, D-85748 Garching, Germany*
(Received 6 May 2013; published 17 July 2013)

The occurrence of low-energy collective motion is a widespread phenomenon in quantum systems. To describe fluctuations about the equilibrium deformation and to understand the nature of excited 0^+ states in deformed nuclei, we improve the many-body wave functions by superimposing angular-momentum-projected states constructed with different quadrupole deformations. We take deformed rare-earth nuclei as examples, compare quantitatively the calculated low-lying 0^+ bands and the associated electric monopole transition matrix elements with experimental data. The analysis of the resulting wave functions for the excited 0^+ states indicates clear features of quantum oscillations, with large fluctuations in deformation for soft nuclei and strong anharmonicities in the oscillations for rigidly deformed nuclei.

DOI: 10.1103/PhysRevC.88.014315 PACS number(s): 24.60.Ky, 21.10.Re, 21.60.Ev, 27.70.+q

I. INTRODUCTION

In many examples of quantum many-body systems, one describes the low-lying spectra in terms of elementary excitation modes corresponding to fluctuations about the equilibrium of the system. The nature of the fluctuations depend on intrinsic properties of the system. A well-known example is molecular physics where the atoms form a relatively rigid structure in the molecule, and the low-energy internal excitations correspond to vibrational modes. In nuclear systems, the modes of interest are collective vibrations of nuclear shape that characterizes the equilibrium configuration. Bohr and Mottelson [1] associated low-lying $I^\pi = 0^+$ and 2^+ excitations with (one-phonon) β- and γ-vibrational modes, where the quantum numbers I and π denote angular momentum and parity of the states. These collective shape oscillations occur in nuclei having in the equilibrium nonspherical quadrupole shapes with the deformation parameters β and γ. In the algebraic models, these vibrational modes are classified so as to belong to the lowest collective excitations of the ground state [2]. Whereas γ vibrations are found systematically across entire regions of deformed nuclei, the experimental identification of β vibrations remains elusive [3]. In particular, the real nature of the second 0^+ states, 0_2^+, has not been fully understood [4,5].

On the theoretical side there is a large number of phenomenological nuclear models, many of which are based on the group theory (for a recent review, see Ref. [3]). There is a lack of microscopic descriptions, mainly because it is difficult to take fully into account all possible microscopic degrees of freedom for heavy, deformed nuclei. A proper microscopic description of collective vibrations in deformation space requires wave functions to be superpositions of states with different deformation conserving the quantum numbers of angular momentum and parity.

The projected shell model (PSM) [6] has been successful in the microscopic description of the yrast properties of rotational nuclei and high-spin bands with multi-quasiparticle (qp) structures. For these studies one usually starts with a fixed deformation of the mean field (with either axial or triaxial symmetry), and the dynamics is obtained through mixing various qp configurations preserving the symmetries. The mixing can be significant for cases of sudden changes in the structure, as for example in regions of band crossings. However, the mixing is often insufficient to produce enough collectivity for states having vibrational character. Conceptually, one might hope that, within the shell-model concept, inclusion of a large amount of 2-qp states with the same deformation could introduce a collective contribution that would produce the desired low-lying vibrational states. But such attempts have failed in practice [7]. Because of the large pairing gap, the energy of the lowest 2-qp state is, in a typical deformed nucleus of the rare-earth region, above 1.5 MeV and is much higher than the actual vibrational band-head energy, which typically lies between 0.5 and 1 MeV. The quadrupole force in the Hamiltonian is apparently too weak to lower the vibrational energy by such a large amount. In fact, calculations including thousands of 2-qp and 4-qp states do not lead to low-lying excited states that look like the low-lying collective states found in experiment [7]. One has to conclude that for a description of β vibrations, the original PSM has not been successful. Therefore, alternative approaches have to be developed [8,9].

II. THE METHOD

The results reported in this paper are obtained by an extension of the original PSM that allows the mixing of product states with different deformation to construct better wave functions. It employs the fully quantum-mechanical generate coordinate method (GCM) [10] based on a very general ansatz for a trial wave function, i.e., a linear superposition of product states $|\Phi(a)\rangle$ depending on a set of (real or complex) parameters $\{a\} = a_1, a_2, \ldots, a_i$ (the so-called generator coordinates):

$$|\Psi\rangle = \int da f(a)|\Phi(a)\rangle. \quad (1)$$

*Corresponding author: sunyang@sjtu.edu.cn

The generating functions $|\Phi(a)\rangle$ in Eq. (1) can be chosen, for example, as Nilsson wave functions [11] with different deformations a of the potential. $f(a)$ in Eq. (1) is the weight function, which is determined by the variational principle, or equivalently, by solving the Hill-Wheeler equation [12]

$$\mathcal{H}f = E\mathcal{N}f, \tag{2}$$

with the overlap functions

$$\begin{aligned}\mathcal{H}(a,a') &= \langle\Phi(a)|\hat{H}|\Phi(a')\rangle,\\ \mathcal{N}(a,a') &= \langle\Phi(a)|\Phi(a')\rangle\end{aligned} \tag{3}$$

as integral kernels.

As in the PSM one superimposes qp states with good symmetries, we use projected states associated with different axial deformation ε_2, and write Eq. (1) as

$$|\Psi^{I,N}\rangle = \int d\varepsilon_2 f^{I,N}(\varepsilon_2)\hat{P}^I\hat{P}^N|\Phi_0(\varepsilon_2)\rangle, \tag{4}$$

where $\hat{P}^I$ and $\hat{P}^N$ are projection operators on good angular-momentum and particle number [10] restoring the rotational symmetry violated in the deformed mean field and the gauge symmetry violated in the BCS approximation. $|\Phi_0(\varepsilon)\rangle$ is a Nilsson + BCS state, the qp vacuum with deformation ε_2.

This method has been used for the investigations of 0^+ excitations also in the context of nonrelativistic [13,14] and relativistic [15] density functional theory (DFT). These are extremely time-consuming calculations, and therefore in many cases additional approximations are used to derive the parameters of a Bohr-Hamiltonian, as for instance the Gaussian overlap approximation (GOA) or adiabatic time-dependent Hartree-Fock (ATDHF) theory [15,16]. Because of the small effective mass in many density functional theories [17] the corresponding single particle spectra deviate considerably from experimental values. The advantage of the present method is its simplicity together with the realistic single particle spectra of the Nilsson model [11] used here.

The Hamiltonian in Eq. (3) is identical to that used in the original PSM [6]

$$\hat{H} = \hat{H}_0 - \frac{\chi}{2}\sum_\mu \hat{Q}^+_\mu\hat{Q}_\mu - G_M\hat{P}^+\hat{P} - G_Q\sum_\mu \hat{P}^+_\mu\hat{P}_\mu, \tag{5}$$

where the residual interaction consists of separable forces of the quadrupole-quadrupole + pairing type, with inclusion of a quadrupole-pairing term. In PSM [6], the strength for the quadrupole-quadrupole interaction χ is usually determined by enforcing the condition that such a force would result in a correct quadrupole deformation in variational calculations. As there are now different deformation points, we take the χ value corresponding to a fixed $\varepsilon_2 = 0.305$. The monopole pairing strengths parameters in Eq. (5) are taken to be $G_M = (G_1 \mp G_2(N-Z)/A)/A$, with the minus sign for neutrons and plus sign for protons. Here we use $G_1 = 21.24$ MeV and $G_2 = 13.86$ MeV for the present mass region as in the original PSM [6]. The strength of quadrupole pairing is, as usual, assumed to be $G_Q = 0.16G_M$. We stress that all the results presented below are obtained by using the same set of parameters. None of them is adjusted to the results shown in the present investigation.

The central task for the numerical calculation is to evaluate the matrix element

$$O^{I,N} = \langle\Phi_0(\varepsilon_2)|\hat{O}\hat{P}^I\hat{P}^N|\Phi_0(\varepsilon_2')\rangle, \tag{6}$$

where $\hat{O}$ is $\hat{H}$ [Eq. (5)] or 1. A description for the computation of $O^{I,N}$ can be found in Ref. [18]. In the actual calculation we consider the deformation range from $\epsilon_2 \approx 0.055$ to 0.455, and take in Eq. (4) discrete values for ϵ_2 in steps of $\Delta\epsilon_2 = 0.05$. The number of mesh points is from 7 to 10, depending on convergence of the results.

III. RESULTS AND DISCUSSIONS

In Fig. 1, we show the results of a systematic calculation for the first excited 0^+_2 state in Gd, Dy, and Er isotopes, and compare them with experimental data. The energy levels 2^+_1, 4^+_1, and 6^+_1 of the ground state rotational band are also shown. We find that with a single set of parameters in the Hamiltonian, the characteristic behavior of the shell evolution is well reproduced. This certainly benefits from the improved GCM wave function of Eq. (4). It is seen that starting from the neutron number $N = 90$ on the left-hand side of Fig. 1 and

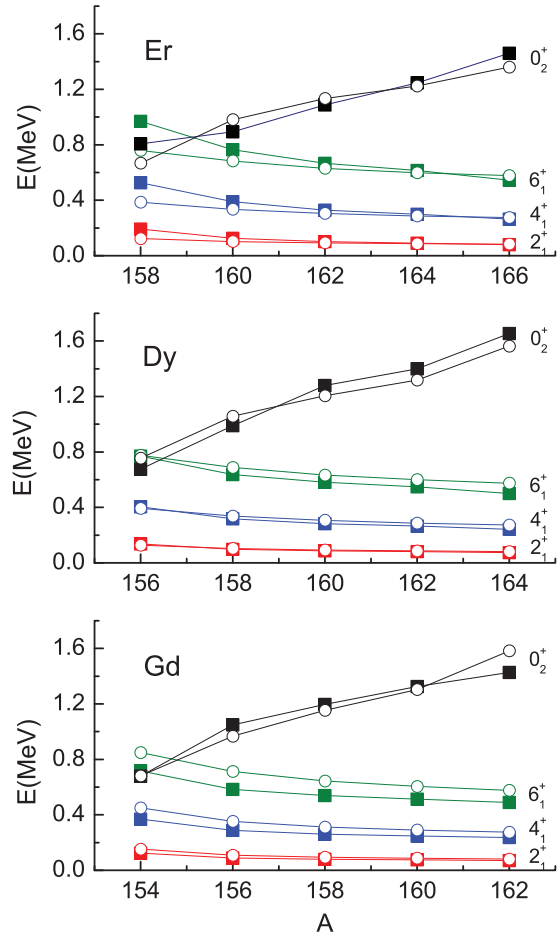

FIG. 1. (Color online) Comparison of calculated 0^+_2 state with experimental data for Gd, Dy, and Er isotopes. The energy levels 2^+_1, 4^+_1, and 6^+_1 of ground-state rotational band are also shown. Calculated results (open circles) are compared with data (filled squares).

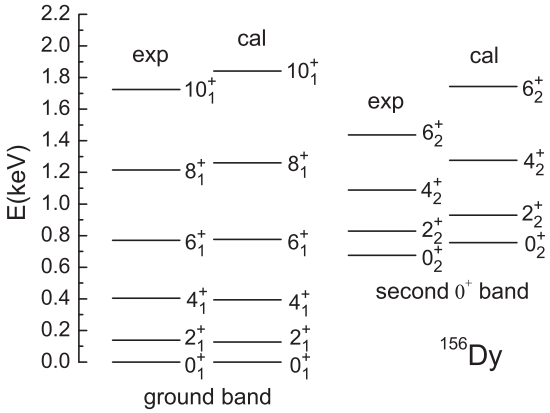

FIG. 2. Calculated energy levels for low-lying states of the ground-state band and second 0^+ band are compared with data.

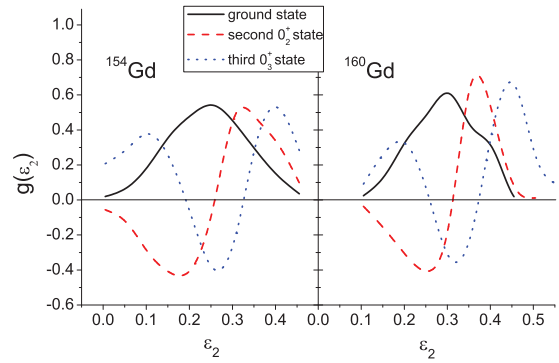

FIG. 3. (Color online) Calculated distribution function of deformation for the first three 0^+ states in ^{154}Gd and ^{160}Gd.

going to heavier isotopes the ground state bands becomes more and more compressed, eventually following the rotational rule of $E \sim I(I+1)$ at $N = 98$. On the other hand, the 0_2^+ state is found low for the isotopes with neutron number 90, which are thought to be soft nuclei with low-energy vibrational states. Without any adjustable parameter, the increase of the energy of the 0_2^+ state with increasing neutron number is correctly reproduced for all three isotopic chains, thus clearly distinguishing the spectral differences of softness in lighter isotopes and stiffness in heavier isotopes, with regard to deformation. The case with the largest discrepancy between calculation and data is ^{158}Er, which is known to be relatively soft in triaxiality, a shape phenomenon that is not a focus of the present work.

To show the description of collectivity, we take in Fig. 2 ^{156}Dy as an example. The present calculation reproduces nearly perfectly the ground band up to spin 10, thus correctly giving the moment of inertia of this nucleus. For the band built on the second 0^+ state, the calculated level separation becomes larger than data with increasing spin. The reason for this discrepancy can be easily speculated. It may possibly be due to the mixing with further qp excitations which may become important for the energy region higher than 1.5 MeV but omitted here. Without the inclusion of this qp mixing, calculations for the third, forth, etc. 0^+ states, as those experimentally found in Ref. [19], may not be realistic.

The results in Figs. 1 and 2 suggest that the GCM approach, with integration of states of different deformations expressed in Eq. (4), has improved the quality of the wave functions considerably. Particularly for soft nuclei, the present results differ qualitatively from those obtained by constructing wave functions with a fixed deformation at the potential minimum, as assumed in the original PSM [6]. This proves that GCM is an efficient way to approach a quantum many-body problem of the current interest. Hara *et al.* [20], by comparing the results of PSM and GCM in a study of high-spin states, concluded that both PSM and GCM are reasonable shell model truncation schemes. The PSM carries out the configuration mixing in terms of qp excitations while GCM in terms of Slater determinants that belong to different nuclear shapes. However, for particular physics problems, the two methods may not to be equally efficient. As we have shown, mixing of 2-qp states, as done in the original PSM, may not be an efficient way to describe the rapid evolution of shape changes studied here.

Because of the general properties of the Hill-Wheeler equation that diagonalizes the Hamiltonian in the nonorthogonal basis of generator states $|\Phi(a)\rangle$ [21], the weight function $f(a)$ in Eq. (1) is not the proper quantity to analyze the GCM wave functions. However, it can be shown [10] that the function

$$g(\varepsilon_2) = \int \mathcal{N}^{1/2}(\varepsilon_2, \varepsilon_2') f(\varepsilon_2') d\varepsilon_2', \tag{7}$$

corresponds to a transformation of $f(\varepsilon_2')$ to an orthogonal basis, and therefore, is a proper representation for the distribution of generator coordinates in the GCM wave functions.

Calculated $g(\varepsilon_2)$ values for ^{154,160}Gd are shown in Fig. 3. It is seen that the curve for the first 0^+ state is Gaussian-like, while the functions $g(\varepsilon_2)$ for the second and the third 0^+ state oscillate. The second 0^+ state has one and the third 0^+ state has two nodes. These forms remind us to a one-dimensional harmonic oscillator given in textbooks [22], with some anharmonicities as discussed below. The first three 0^+ states shown here correspond to the ground state and the lowest two vibrational excitations (one phonon and two phonon states) in a one-dimensional harmonic oscillator potential characterized by the coordinate ε_2.

Normalized probability distribution function $g^2(\varepsilon_2)$ for the ground state 0_1^+ and the excited 0_2^+ state are shown in Fig. 4. For the 0_1^+ state, it exhibits, as expected, a beautiful Gaussian shape centered at the minimum of the energy surface, where the ground-state deformation may be defined. The deformation can be directly read from the figure as $\varepsilon_2 = 0.25$ for ^{154}Gd and $\varepsilon_2 = 0.30$ for ^{160}Gd, respectively. The distribution is wider for ^{154}Gd, reflecting the softness of this nucleus. Quite differently, $g^2(\varepsilon_2)$ for the 0_2^+ state are much extended, with a distribution minimum, instead of a maximum, at the ground-state deformation. The dip in the 0_2^+ state corresponds to a node in the corresponding wave function (see Fig. 3). There is not one, but two separate peaks in the $g^2(\varepsilon_2)$ curve corresponding to the enhanced probability at the turning points of the oscillation. Obviously, the distribution

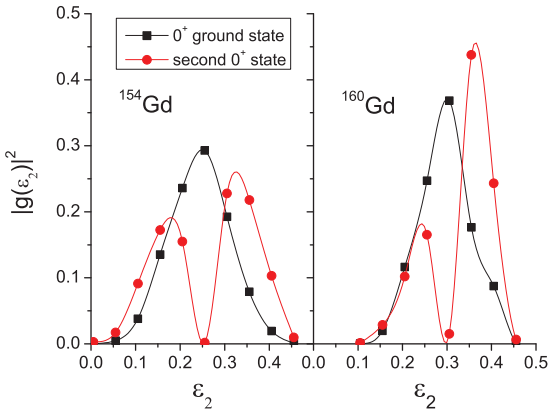

FIG. 4. (Color online) Calculated probability function of deformation for the ground state 0_1^+ and the excited 0_2^+ state in ^{154}Gd and ^{160}Gd. Symbols correspond to the discrete deformations used for the integration in Eq. (4).

in deformation for the 0_2^+ states is much more fragmented, reflecting a vibrational nature of these states.

The distribution function $g^2(\varepsilon_2)$ describes the probability that the nucleus has the deformation ε_2. The picture shown in Fig. 4 clearly distinguishes the two 0^+ states. While for the 0_1^+ ground state, the system stays mainly at system's deformation with the largest probability, such a probability for the 0_2^+ state is very small. For the 0_2^+ state, that the two peaks having different heights lie separately at both sides of the equilibrium indicates an anharmonic oscillation. Our calculation suggests a stronger anharmonicity for the excited 0_2^+ state in the strongly deformed ^{160}Gd. The anharmonicity increases with neutron number because of the increasing excitation energy, where the potential deviates more from an ideal quadratic shape. Interestingly, the system prefers to have a larger probability in the site of larger deformation, as the peak height at $\varepsilon_2 \approx 0.38$ is obviously higher. Moreover, the distance from a peak to the equilibrium measures the average deviation from the equilibrium. The fact that the distance is larger for ^{154}Gd indicates again the softness of this isotope.

Another observable that probes the structure of these states is the matrix element of electric monopole transition, $\langle \Psi_f^I | \hat{T}(E0) | \Psi_i^I \rangle$, from the members of the excited 0^+ band (labeled as i) to those of the ground-state band (labeled as f) and connected by the $E0$ operator defined as

$$\hat{T}(E0) = e_\pi \sum_\pi r_\pi^2 + e_\nu \sum_\nu r_\nu^2. \tag{8}$$

In Eq. (8), π and ν run over single protons and neutrons, respectively, and $e_\pi = 1.5e$ and $e_\nu = 0.5e$ are the effective charges in the model. These effective charges are introduced as the model has a core of 40 neutrons and 20 protons. We employ the 'standard' values for the effective charges that describe $B(E2)$ transitions properly [6]. However, we are aware that these values may not be the best ones for $E0$ transitions.

In Table I, we compare the calculated $E0$-matrix elements for isotopes for which experimental data are available. The data are converted from the $\rho^2(E0)$ values in Refs. [23,24]. It can be seen that our calculation describes the data reasonably well. In particular, with increasing masses, the decreasing trend in $E0$ transition for the isotopes studied here is correctly reproduced. Our numerical results indicate that the calculated difference of these matrix elements for the spin states with $I = 0$ and 2 (see ^{154,156}Gd) is very small, consistent with the general understanding that the electric monopole transition is in principle independent of angular momentum [1,23]. The small differences found in our calculations are possibly caused by variations in the wave functions due to rotation. We note that the calculations within the interacting boson model [25] gave a large difference between the spin states with $I = 0$ and 2. The most recent calculation within the CHFB + 5DCH theory [16] globally overestimated the E0 strengths by an order of magnitude. The authors in Ref. [16] pointed out that the disagreement with data is not uncommon but occurs also in other models of nuclear structure. For example, enforcing realistic model descriptions of $M1$ and $E2$ transitions or charge radii, it is a usual consequence that calculated $E0$ strengths are up to 10 times stronger than the experimental values [25–27].

TABLE I. Comparison of the calculated $E0$-matrix elements (in e fm^2) with experimental data [23,24].

Isotope	$I_i^+ \to I_f^+$	Cal.	Exp.
^{154}Gd	$0_2^+ \to 0_1^+$	8.40	12(2)
	$2_2^+ \to 2_1^+$	8.41	11(1)
^{156}Gd	$0_2^+ \to 0_1^+$	6.73	8.6(21)
	$2_2^+ \to 2_1^+$	6.64	9.8(5)
^{158}Gd	$2_2^+ \to 2_1^+$	5.27	<2
^{158}Dy	$2_2^+ \to 2_1^+$	5.82	6.9(16)
^{160}Dy	$2_2^+ \to 2_1^+$	4.67	5.5(7)
^{164}Er	$2_2^+ \to 2_1^+$	4.55	3.1(8)
^{166}Er	$0_2^+ \to 0_1^+$	3.82	2.0(5)

IV. CONCLUSION

In order to describe shape fluctuations around the deformation equilibrium in deformed nuclei, we improved the nuclear many-body wave functions by superimposing angular-momentum- and number-projected states constructed with different quadrupole deformation parameters. We calculate the low-lying collective 0^+ states in deformed rare-earth nuclei and analyze the obtained wave functions in detail. It has been found that these states exhibit clear features of quantum oscillations, with large fluctuations in deformation found for soft nuclei and strong anharmonicities for rigidly deformed nuclei. Associated electric monopole matrix elements have also been calculated. The results compare reasonably well with available experimental data. With a single set of parameters, the characteristic features of qualitatively different systems can be distinguished by the resulting distribution functions, thus providing new microscopic insight for the traditional collective states in nuclei.

The present calculations are restricted to axial symmetry. The inclusion of triaxial deformations is in principle possible, but it goes beyond the scope of this investigation. Therefore,

so far, γ-vibrations are not included and the open question of admixtures of 2γ configurations in the 0_2^+ state (see Ref. [28]) cannot be answered yet. Work in this direction is in progress.

Finally, we stress that although our discussion has been restricted to nuclear systems, the same many-body technique employed here is applicable to many other fields of physics where quantum fluctuations are important.

ACKNOWLEDGMENT

Valuable discussions with G. Bertsch are acknowledged. This work was supported by the National Natural Science Foundation of China (Nos. 11135005 and 11075103), by the 973 Program of China (No. 2013CB834401), and by the DFG Cluster of Excellence "Origin and Structure of the Universe" (www.universe-cluster.de).

[1] A. Bohr and B. R. Mottelson, *Nuclear Structure* (W. A. Benjamin, Inc., New York, 1975).
[2] F. Iachello, Phys. Rev. Lett. **53**, 1427 (1984).
[3] J. L. Wood, J. Phys. Conf. Ser. **403**, 012011 (2012).
[4] P. E. Garrett, J. Phys. G: Nucl. Part. Phys. **27**, R1 (2001).
[5] J. Terasaki and J. Engel, Phys. Rev. C **84**, 014332 (2011).
[6] K. Hara and Y. Sun, Int. J. Mod. Phys. E **4**, 637 (1995).
[7] Y. Sun (unpublished).
[8] J. L. Egido, H. J. Mang, and P. Ring, Nucl. Phys. A **339**, 390 (1980).
[9] Y. Sun and C.-L. Wu, Phys. Rev. C **68**, 024315 (2003).
[10] P. Ring and P. Schuck, *The Nuclear Many-body Problem* (Springer-Verlag, New York, 1980).
[11] S. G. Nilsson, Mat. Fys. Medd. Dan. Vidensk. Selsk **29**, 16 (1955).
[12] D. J. Hill and J. A. Wheeler, Phys. Rev. **89**, 1102 (1953).
[13] T. R. Rodríguez and J. L. Egido, Phys. Lett. B **705**, 255 (2011).
[14] J. M. Yao, M. Bender, and P.-H. Heenen, Phys. Rev. C **87**, 034322 (2013).
[15] Y. Fu, H. Mei, J. Xiang, Z. P. Li, J. M. Yao, and J. Meng, Phys. Rev. C **87**, 054305 (2013).
[16] J.-P. Delaroche, M. Girod, J. Libert, H. Goutte, S. Hilaire, S. Péru, N. Pillet, and G. F. Bertsch, Phys. Rev. C **81**, 014303 (2010).
[17] E. Litvinova and P. Ring, Phys. Rev. C **73**, 044328 (2006).
[18] Y. Sun, Rev. Mex. Fis. S **54**, 122 (2008).
[19] S. R. Lesher, A. Aprahamian, L. Trache, A. Oros-Peusquens, S. Deyliz, A. Gollwitzer, R. Hertenberger, B. D. Valnion, and G. Graw, Phys. Rev. C **66**, 051305(R) (2002).
[20] K. Hara, Y. Sun, and T. Mizusaki, Phys. Rev. Lett. **83**, 1922 (1999).
[21] C. W. Wong, Nucl. Phys. A **147**, 545 (1970).
[22] D. J. Griffiths, *Introduction to Quantum Mechanics* (Pearson Prentice Hall, Saddle River, NJ, 2005).
[23] J. L. Wood, E. F. Zganjar, C. De Coster, and K. Heyde, Nucl. Phys. A **651**, 323 (1999).
[24] T. Kibedi and R. H. Spear, At. Data Nucl. Data Tables **89**, 77 (2005).
[25] S. Zerguine, P. Van Isacker, A. Bouldjedri, and S. Heinze, Phys. Rev. Lett. **101**, 022502 (2008).
[26] K. Takada and S. Tazaki, Nucl. Phys. A **395**, 165 (1983), and references therein.
[27] J. Bonnet, A. Krugmann, J. Beller, N. Pietralla, and R. V. Jolos, Phys. Rev. C **79**, 034307 (2009).
[28] R. F. Casten and P. von Brentano, Phys. Rev. C **51**, 3528 (1995), and references therein.